The Design and Realization of a Hyper-Chaotic Circuit Based on a Flux-Controlled Memristor with Linear Memductance

Article *in* Journal of Circuits, Systems and Computers · March 2018

DOI: 10.1142/S021812661850038X

CITATIONS
2

READS
38

3 authors, including:

Chunhua Wang
Hunan University
167 PUBLICATIONS **792** CITATIONS

SEE PROFILE

Journal of Circuits, Systems, and Computers
Vol. 27, No. 3 (2018) 1850038 (17 pages)

DOI: 10.1142/S021812661850038X

World Scientific
www.worldscientific.com

The Design and Realization of a Hyper-Chaotic Circuit Based on a Flux-Controlled Memristor with Linear Memductance*

Chunhua Wang†, Ling Zhou‡ and Renping Wu§

College of Information Science and Engineering, Hunan University, Changsha 410082, P. R. China
†*wch1227164@hnu.edu.cn*
‡*64493645@qq.com*
§*250546453@qq.com*

Received 3 December 2015
Accepted 6 June 2017
Published 7 July 2017

In this paper, a flux-controlled memristor with linear memductance is proposed. Compared with the memristor with piecewise linear memductance and the memristor with smooth continuous nonlinearity memductance which are widely used in the study of memristive chaotic system, the proposed memristor has simple mathematical model and is easy to implement. Multisim circuit simulation and breadboard experiment are realized, and the memristor can exhibit a pinched hysteresis loop in the voltage–current plane when driven by a periodic voltage. In addition, a new hyper-chaotic system is presented in this paper by adding the proposed memristor into the Lorenz system. The transient chaos and multiple attractors are observed in this memristive system. The dynamical behaviors of the proposed system are analyzed by equilibria, Lyapunov exponents, bifurcation diagram and phase portrait. Finally, an electronic circuit is designed to implement the hyper-chaotic memristive system.

Keywords: Memristor; emulator; hyper-chaotic; electronic circuit.

1. Introduction

From the circuit-theoretic point of view, there are four fundamental circuit variables, namely, current i, the voltage v, charge q and flux-linkage φ. Three relationships are given, respectively, by the axiomatic definition of the three classical circuit elements, namely, the resistor (defined by a relationship between v and i), the inductor (defined by a relationship between φ and i), and the capacitor (defined by a relationship between q and v). In 1971, Chua[1] postulated the existence of a fourth basic two-terminal circuit element called the memristor, which defined by a

*This paper was recommended by Regional Editor Emre Salman.
†Corresponding author.

relationship between charge q and flux-linkage φ. In 2008, Strukov and others in HP lab[2,3] using nanoscale technology firstly fabricated a physical memristor, which is a two-terminal electrical device based on TiO2 material. Thus, the memristor's place as the fourth fundamental circuit element was cemented. Memristor, as the fourth fundamental circuit element, with memory and nonlinear characteristics, has potential application in those fields: artificial intelligence, nonvolatile impedance memory, field programmable gate array, neural network and spin electronic devices.[4–10]

In addition, memristor, which is a nonlinear element with small size and low power consumption, is a good choice for the study of chaotic circuit. More and more chaotic circuits based on memristor have been proposed[12–25] since the first memristor-based chaotic circuit was proposed by Itoh and Chua[11] in 2008. After reading these literatures, we find that almost all memristive chaotic systems are based on the memristor with piecewise linear memductance[12–18] or based on the memristor with smooth continuous nonlinearity memductance.[19–25] Is there any other simple choice to study memristive chaotic circuit?

In this paper, a flux-controlled memristor with linear memductance is proposed and then an emulator is presented. The memristor with linear memductance,which makes the memristor's mathematical model more simple and easy to implement,is different from those above mentioned.[12–25] We use only one Multiplier and two Op-amps in the emulator which has lesser elements than the emulators.[17–25]

By using the memristor proposed in this paper, we proposed a new 4D hyper-chaotic circuit. Hyper-chaotic system has more complex dynamics, which can be widely applied in many realms such as cryptosystem, neural network, and secure communication. However, the memristive systems are all chaotic.[12–23] Although the hyper-chaotic systems are proposed in Refs. 24 and 25, the memductance function of these memristive systems is two-order function. It is interesting to generate hyper-chaotic attractor by using simple linear memductance.

Multiple attractors are an interesting topic, which are reported by many researchers.[29,30] The various coexisting attractors can have quite different properties such as Lyapunov exponents, and the occurrences in all combinations: fixed points, limit cycles, torus, chaotic attractors, and hyperchaotic attractors.[29] In this paper, we found the coexisting transient chaotic attractors and chaotic attractors.

This paper is organized as follows. In Sec. 2, a memristor with linear memductance is proposed, and an emulator built from off-the-shelf solid state components which imitates the behavior of the proposed memristor presented. In Sec. 3, the hyper-chaotic circuit is described and the hyper-chaotic dynamics are confirmed by numerical computation. In Sec. 4, multiple chaotic attractors and transient chaotic attractors are discussed. In Sec. 5, an electronic circuit is designed to implement the hyper-chaotic circuit. Finally, the conclusions are given in Sec. 6.

2. The Flux-Controlled Memristor with Linear Memductance and Emulator

Memristor is the fourth basic two-terminal circuit element besides resistor, inductor, and capacitor, which describes the relationship between the charge q and the flux-linkage φ. According to Chua,[1] a flux-controlled memristor is defined by the relation of the type $g(\varphi, q) = 0$ and this relation can be expressed as a single-valued function of the flux-linkage φ. The current of a flux-controlled memristor is given by

$$i = W(\varphi)v\,, \tag{1}$$

where $W(\varphi) = dq(\varphi)/d\varphi$. The function $W(\varphi)$ is called the memductance.

Now, we define a flux-controlled memristor as

$$q(\varphi) = a\varphi^2\,, \tag{2}$$

where $a > 0$. According to Eq. (2), we get the memductance

$$W(\varphi) = \frac{dq(\varphi)}{d\varphi} = \beta\varphi\,, \tag{3}$$

where $\beta = 2a > 0$. The current of this memristor is given by

$$i = W(\varphi)v = \beta\varphi v\,. \tag{4}$$

The instantaneous power dissipated by the memristor is given by

$$p = vi = W(\varphi)v^2\,. \tag{5}$$

If the memductance $W(\varphi) \geq 0$, then $p \geq 0$, the memristor is obviously passive.

In comparison with the memristors presented in the papers,[11–23,25,26] our proposed memductance $W(\varphi) = \beta\varphi$ only contains a linear term and no constant term. The intention is to make the mathematical model more simple and make the emulator easier to be implemented.

The emulator schematic is depicted in Fig. 1.

With the properties of Op-amp TL082, Multiplier AD633 and Current Feedback Operational Amplifier AD844 (refer to the datasheet for further information), we can

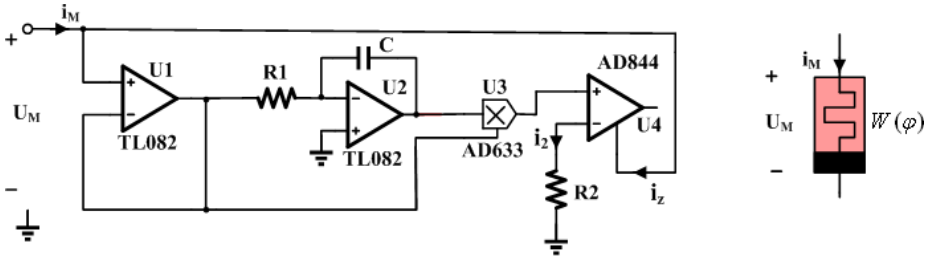

Fig. 1. Schematic of the emulator.

see that U4 is the current-inverter that implements

$$i_M = i_Z = -i_2 = -\frac{v_3}{R_2}\,. \tag{6}$$

Multiplier U3 implements

$$v_3 = v_2 v_1\,. \tag{7}$$

Op-amp U2 implements

$$v_2 = -\int \frac{v_1}{R_1 C} dt\,. \tag{8}$$

Op-amp U1 implements

$$v_1 = v_M\,. \tag{9}$$

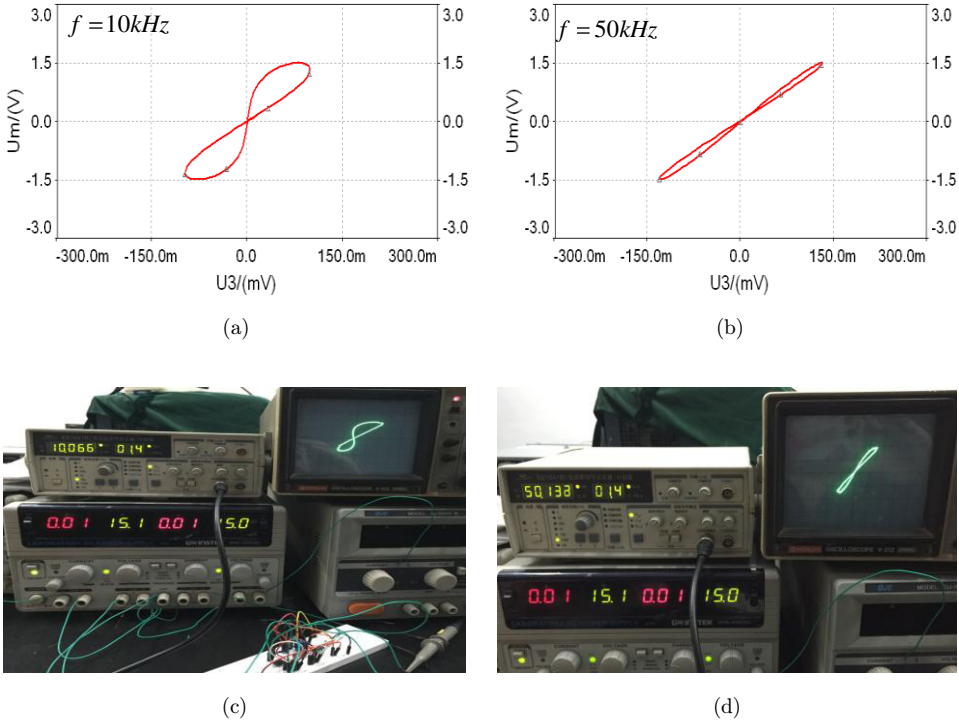

Fig. 2. The $i - v$ characteristics of the proposed memristor. The excited signal is a sinusoid voltage with 1.5 V amplitude. (a) and (b) are the Multisim circuit simulations with a frequency of 10 kHz and 50 kHz. (c) and (d) are the corresponding circuit experiment results. Note that from Eq. (6), we known $i_M = -v_3/R_2$. In order to conveniently measure the current i_M, we use the voltage v_3 substitute the current i_M, which just take a transformation of $1/R_2$ scale.

From Eqs. (6)–(8), we can get

$$i_M = \frac{v_1}{R_1 R_2 C} \int v_1 dt \,. \tag{10}$$

From Eqs. (9) and (10), It is easy to obtain

$$i_M = \frac{v_M}{R_1 R_2 C} \int v_M dt \,. \tag{11}$$

Now, consider the above proposed memristor in Eq. (4). We have $i = i_M$, $v = v_M$, $\varphi = \int v_M \, dt$ (the internal state of the memristor), $\beta = 1/R_1 R_2$C. It can be seen that the circuit indeed realizes the above proposed memristor. And we use the Current Feedback Operational Amplifier AD844 to realize the current-inverter, which makes the design more easy and more direct. Moreover, in the design of emulator, we only use one Multiplier, which makes the design method simpler than others proposed by papers.[17–23]

When $R_1 = 10\,\text{k}$, $R_2 = 1\,\text{k}$, $C = 40\,\text{nF}$, the circuit experiment results of $i_M - v_M$ relationship as shown in Figs. 2(c) and 2(d) are well consistent with the results of the Multisim simulation shown in Figs. 2(a) and 2(b). From the simulations and experiment results, we found that our proposed memristor emulator has a higher frequency range than the reported are.[26–28]

3. The Hyper-Chaotic Circuit Based on Flux-Controlled Memristor with Linear Memductance

Lorenz system is the first chaotic system, which was proposed by Edward Lorenz in 1963. The Lorenz system is a system with three ordinary differential equations

$$\begin{cases} \dot{x} = a(y - x) \,, \\ \dot{y} = cx - y - xz \,, \\ \dot{z} = -bz + xy \,. \end{cases} \tag{12}$$

When the system parameters are taken as $a = 10$, $b = 8/3$, and $c = 30$, the system exhibits chaotic behavior. The phase portraits of Lorenz system are shown in Fig. 3 (the initial condition $x(0) = 0.1$, $y(0) = 0.1$, $z(0) = 0.1$).

By adding the proposed memristor to Lorenz system, a four-dimensional hyper-chaotic system is designed. The schematic is shown in Fig. 4.

The dynamic equations of the circuit in Fig. 4 are

$$\begin{cases} C_x \dot{x} = y/R_1 - x/R_2 \,, \\ C_y \dot{y} = x/R_3 - y/R_5 - xz/R_4 - W(\varphi)x \,, \\ C_z \dot{z} = -z/R_{11} + xy/R_{10} \,, \\ \dot{\varphi} = x \,. \end{cases} \tag{13}$$

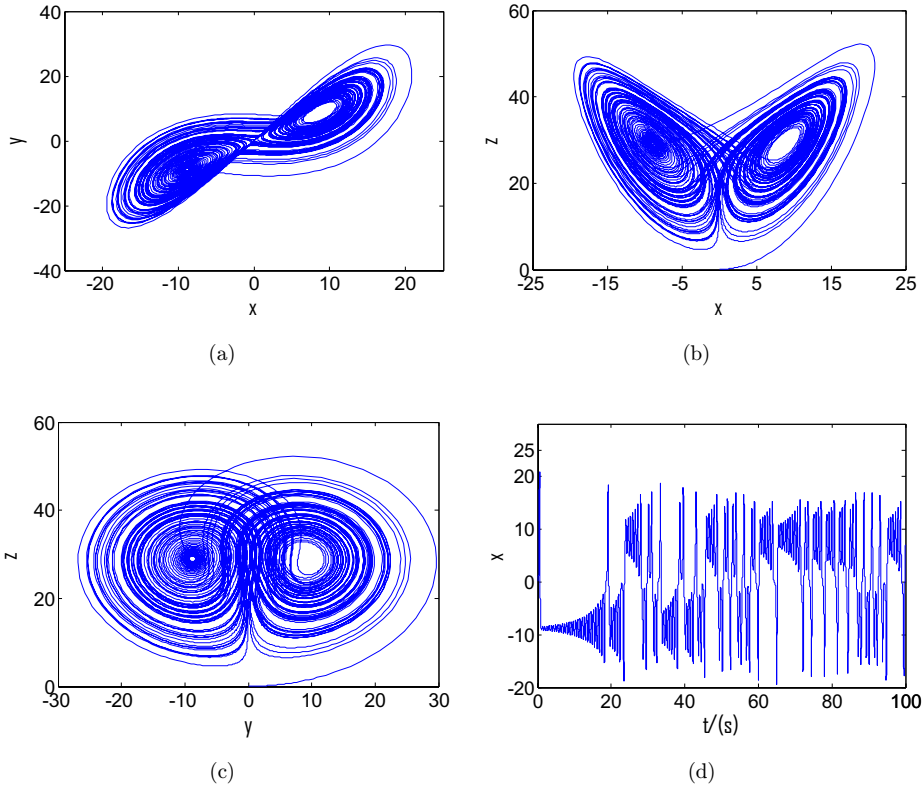

Fig. 3. Phase portraits of Lorenz system. (a) Projection on x–y plane. (b) Projection on x–z plane. (c) Projection on y–z plane. (d) Time-domain waveform of variable x.

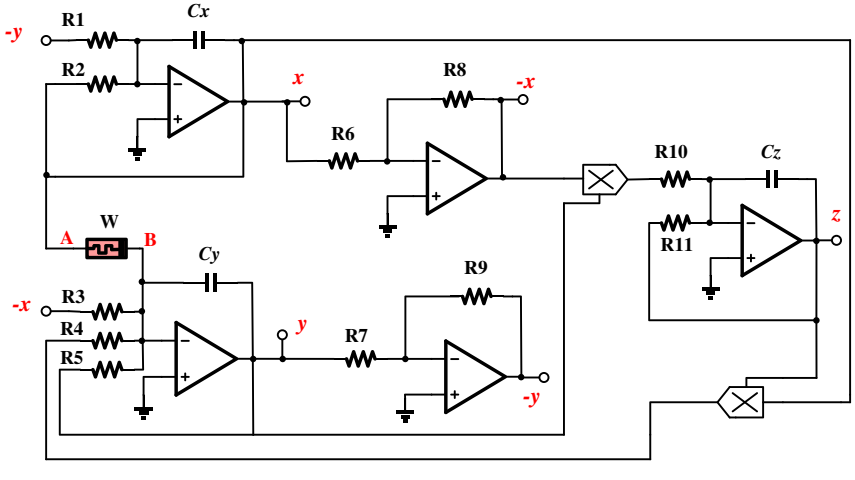

Fig. 4. Schematic of a hyper-chaotic circuit based on the proposed memristor.

We have

$$a = 1/(R_1C_x) = 1(R_2C_x), b = 1/(R_{11}C_z), c = 1/(R_3C_y), R_5C_y = R_4C_y = R_{10}C_z = 1$$

Equation (13) can be described as the following dimensionless equations:

$$\begin{cases} \dot{x} = a(y - x)\,, \\ \dot{y} = cx - y - xz - W(\varphi)x\,, \\ \dot{z} = -bz + xy\,, \\ \dot{\varphi} = x\,, \end{cases} \tag{14}$$

where the memductance function $W(\varphi) = \beta\varphi$. We have $a = 10,\ b = 8/3,\ c = 30,$ $\beta = 0.5$. The divergence of system (14) is given by

$$\nabla V = \frac{\partial \dot{x}}{\partial x} + \frac{\partial \dot{y}}{\partial y} + \frac{\partial \dot{z}}{\partial z} + \frac{\partial \dot{\varphi}}{\partial \varphi} = -a - 1 - b\,.$$

Since $a = 10$, $b = 8/3$, $-a - 1 - b = -13.67 < 0$, the system (14) is dissipative.

3.1. *Equilibria and stability*

The equilibria of system (14) can be derived by solving the following equations:

$$\begin{cases} a(y - x) = 0\,, \\ cx - y - xz - W(\varphi)x = 0\,, \\ -bz + xy = 0\,, \\ x = 0\,. \end{cases} \tag{15}$$

As can be seen, the equilibrium states of system (14) only rely on x, y and z, and are independent from φ. The hyper-chaotic system has the unusual feature of having a line of equilibrium. The equilibria of system (14) can be described as

$$O = \{(x, y, z, \varphi) | x = y = z = 0, \varphi = d\}\,.$$

The Jacobian matrix of system (14) on this line equilibrium is

$$J_O = \begin{bmatrix} -a & a & 0 & 0 \\ c - \beta d & -1 & 0 & 0 \\ 0 & 0 & -b & 0 \\ 1 & 0 & 0 & 0 \end{bmatrix}. \tag{16}$$

The four eigenvalues of matrix J_0 are

$$0, -b, (-(a + 1) \pm \sqrt{(a - 1)^2 - 4a(\beta d - c)})/2\,.$$

If $a = 10$, $b = 8/3$, $c = 30$, $\beta = 0.5$, the four eigenvalues are

$$\lambda_1 = 0, \quad \lambda_2 = -8/3, \quad \lambda_3 = (-11 + \sqrt{1281 - 20d})/2,$$

$$\lambda_4 = (-11 - \sqrt{1281 - 20d})/2\,.$$

When $d > 58$, $\lambda_3 > 0$, $\lambda_4 < 0$, there are one positive eigenvalue, one zero eigenvalue and two negative eigenvalues, and the line equilibrium of system (14) is unstable saddle points. When $d < 58$, $\lambda_3 < 0$, $\lambda_4 < 0$, there are one zero eigenvalue and three negative eigenvalues, and the line equilibrium of system (14) is stable. Since there is no imaginary eigenvalue in J_0, a Hopf bifurcation does not exist near the line equilibrium of system (14).

3.2. *Lyapunov spectrum and bifurcation diagram*

To explore the nonlinear dynamics of this hyper-chaotic circuit, the Lyapunov spectrum and bifurcation diagram of the system (14) are calculated in this section. When $a = 10$, $b = 8/3$, $c = 30$, and β increases from 0 to 0.8 with a step size 0.01, the corresponding Lyapunov exponents of the system (14) can be computed by the QR decomposition-based method,[28] as shown in Fig. 5. Note that when $\beta = 0.5$,

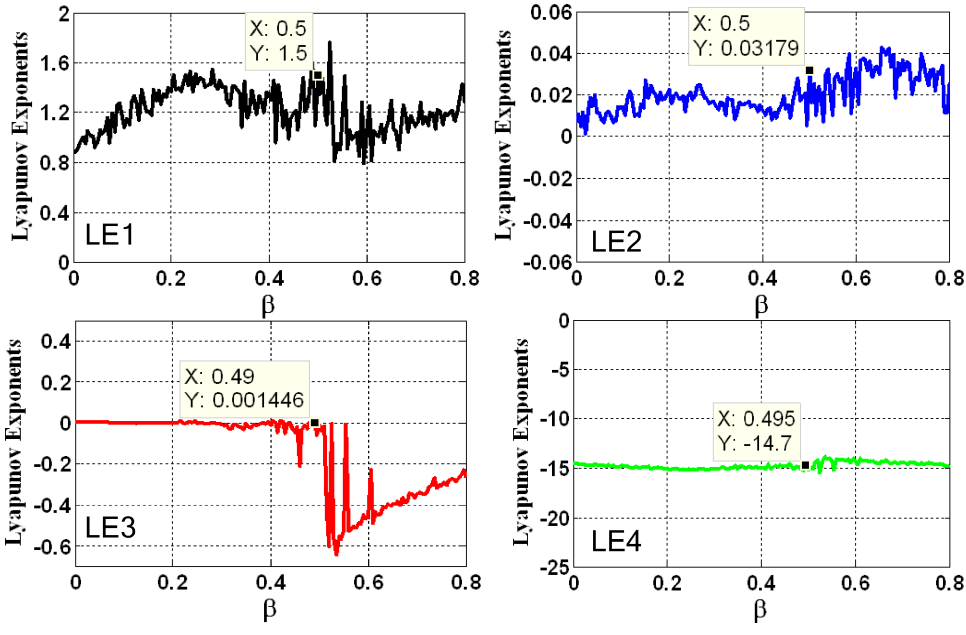

Fig. 5. Lyapunov exponents versus parameter β of system (14) calculated by QR decomposition-based method.

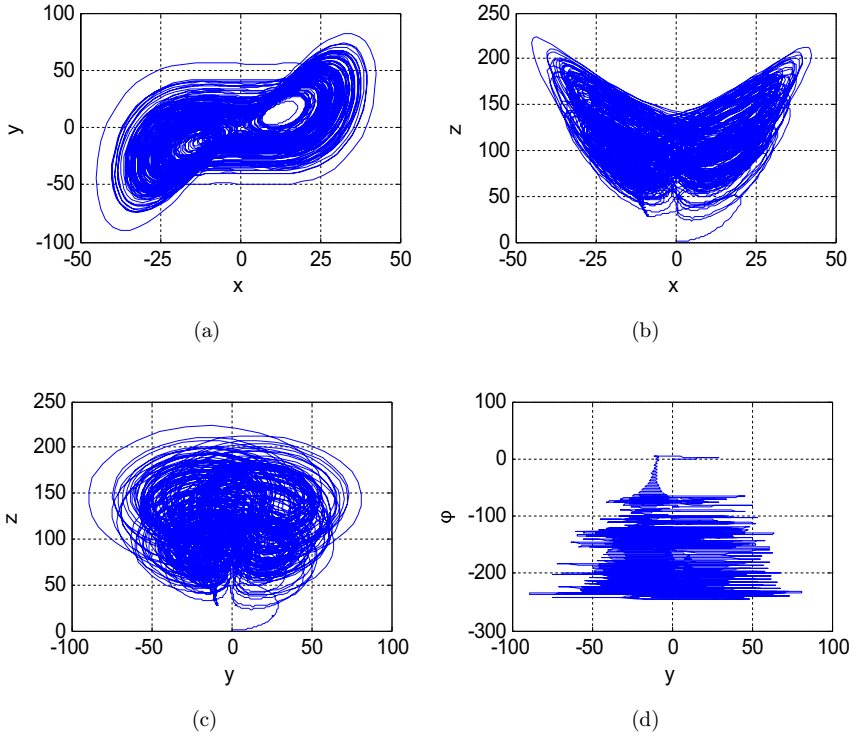

Fig. 6. Hyper-chaotic phase portraits of system (14) with parameter $\beta = 0.5$. (a) Projection on x–y plane. (b) Projection on x–z plane. (c) Projection on y–z plane. (d) Projection on y–φ plane.

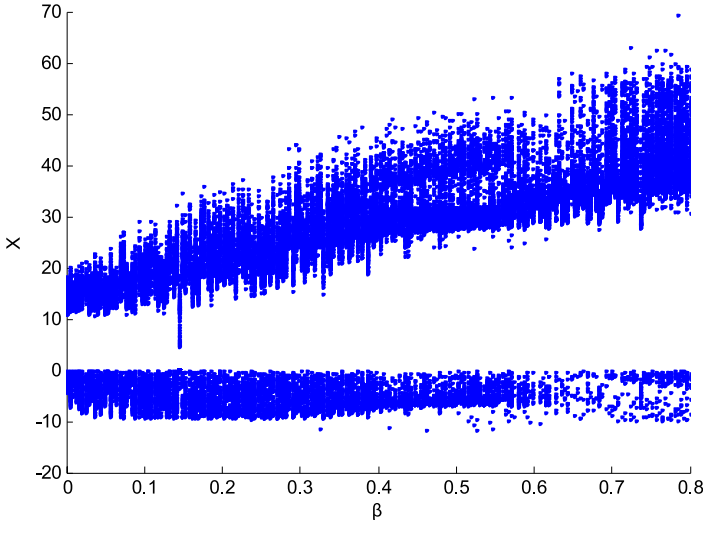

Fig. 7. Bifurcation diagram for increasing parameter β.

the corresponding Lyapunov exponents are: $LE_1 = 1.501$, $LE_2 = 0.0318$, $LE_3 = 0.0014$, $LE_4 = -14.7$. There are two positives, one zero and one negative Lyapunov exponents, which means the system is a hyper-chaotic system. The phase portrait for $\beta = 0.5$ with initial condition (0.1, 0.1, 0.1, 0.1) is depicted in Fig. 6. In order to be sure that the system is truly hyper-chaotic when $\beta = 0.5$, we compute the Lyapunov exponents with the Wolf method[29] which coincide well with the results of QR decomposition-based method. The bifurcation diagram of state variable β with increase of β with a step size 0.01 is given in Fig. 7, which matches the Lyapunov exponents in Fig. 5 very well. The above analysis suggests that the adding of memristor makes the system demonstrate abundant interesting nonlinear phenomena. The memristive hyper-chaotic system with a line of equilibrium could be a novel type of dynamical system.

4. Multiple Attractors

In the following, we take account of the influence of parameter a. The parameters are taken as $b = 8/3$, $c = 30$, and $\beta = 0.5$, and the parameter a is variable. The complex dynamics (chaotic attractors, transient chaotic attractors, hyperchaotic attractors, multiple attractors) are found in this case, and the LEs versus parameter a of system (14) are depicted in Fig. 9.

The coexistence of multiple attractors is one of the most striking phenomena encountered in nonlinear dynamical systems. If the parameters are taken as $a = 13.9$, $b = 8/3$, $c = 30$, and β =0.5, the multiple attractors can be observed as shown Fig. 8. In order to verify the coexistence of multiple attractors, the time sequences (Fig. 10) and LEs (Fig. 11) are calculated.

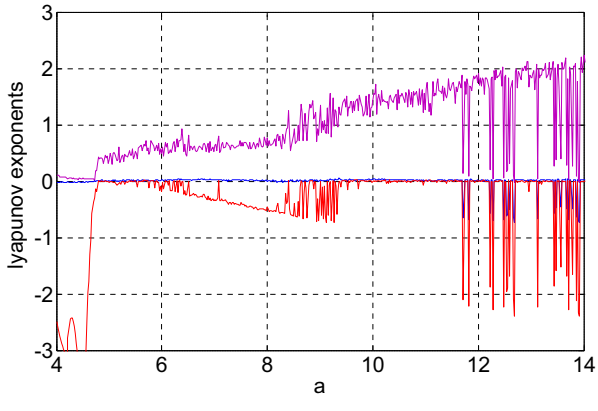

Fig. 8. LEs versus parameter a of system (14).

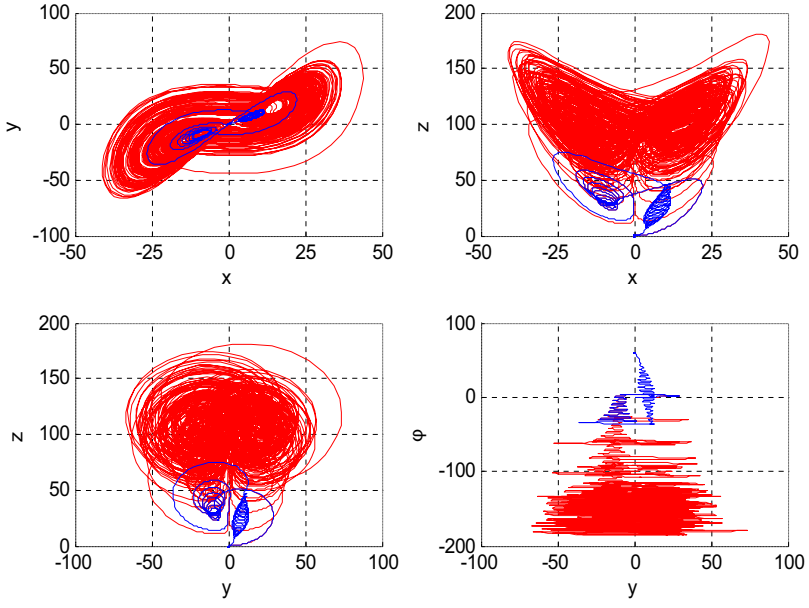

Fig. 9. The phase portraits of system (14) when the parameters are taken as $a = 13.9$, $b = 8/3$, $c = 30$, and $\beta = 0.5$ under different initial condition: the initial condition is [0.1 0.1 0.1 0.1] (blue), the initial condition is [0.1 1 0.1 0.1] (red) (color online).

From Figs. 10 and 11, it can observe that the transient chaos appears when the initial condition is [0.1 0.1 0.1 0.1], while chaotic attractor is found in the initial condition [0.1 1 0.1 0.1].

When a is changing, we can find different attractors when the parameter a is 4. The LEs are 0.102207, −0.017539, −2.494561, and −5.252756. The phase portraits of system (14) are depicted in Fig. 12.

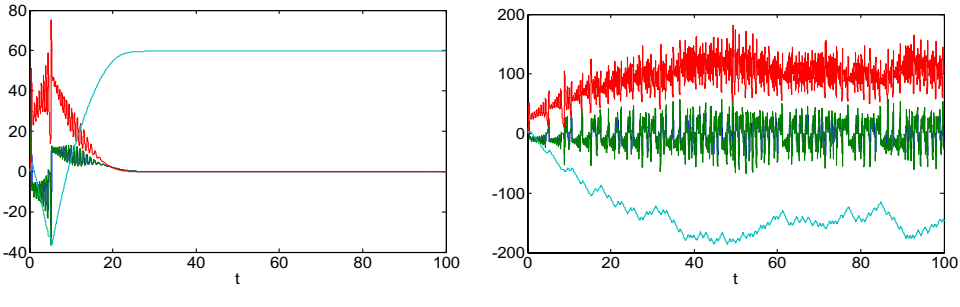

(a) (b)

Fig. 10. The time sequences of system (14) when the parameters are taken as $a = 13.9$, $b = 8/3$, $c = 30$, and $\beta = 0.5$ under different initial condition: (a) the initial condition is [0.1 0.1 0.1 0.1], (b) the initial condition is [0.1 1 0.1 0.1].

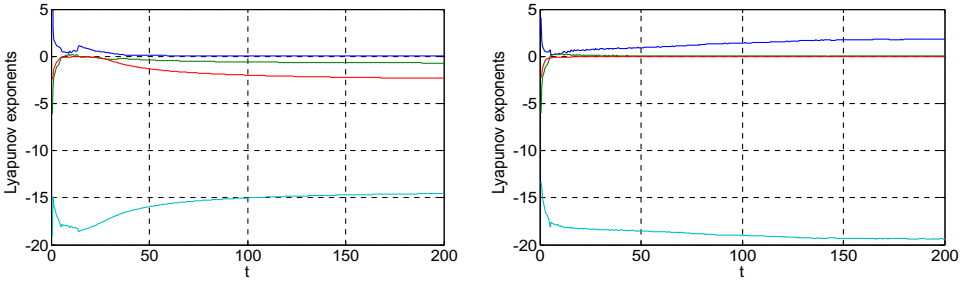

(a) (b)

Fig. 11. The LEs of system (14) versus time t when the parameters are taken as $a = 13.9$, $b = 8/3$, $c = 30$, and $\beta = 0.5$ under different initial condition: (a) the initial condition is [0.1 0.1 0.1 0.1], (b) the initial condition is [0.1 1 0.1 0.1].

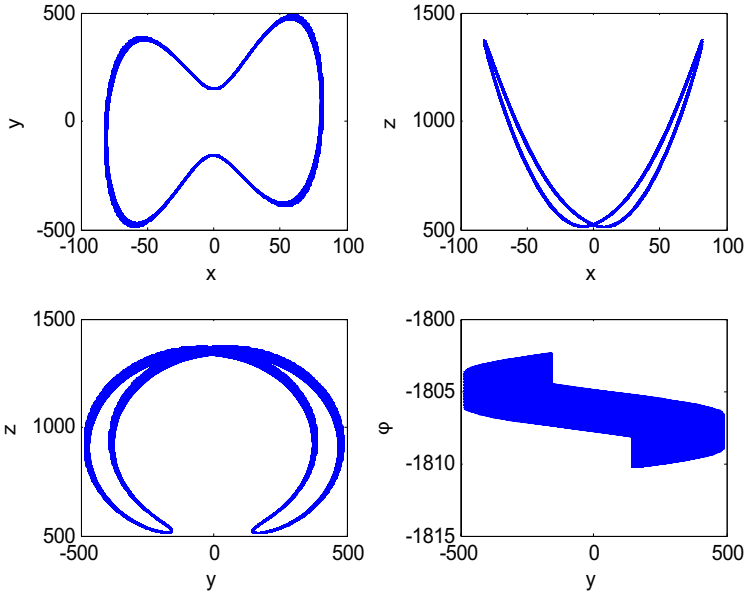

Fig. 12. The phase portraits of system (14) when the parameters are taken as $a = 4$, $b = 8/3$, $c = 30$, and $\beta = 0.5$.

5. Circuit Implementation

It is important to realize the hyper-chaotic systems by the physical circuit before the hyper-chaotic systems are applied in engineering applications. In this section, the memristive hyper-chaotic system (14) is realized by an electronic circuit shown in Fig. 13. The voltages of C_x, C_y, C_z, and C_φ are used as x, $y$and z, and φ, respectively. The operational amplifiers TL082 and the associated circuits perform the basic

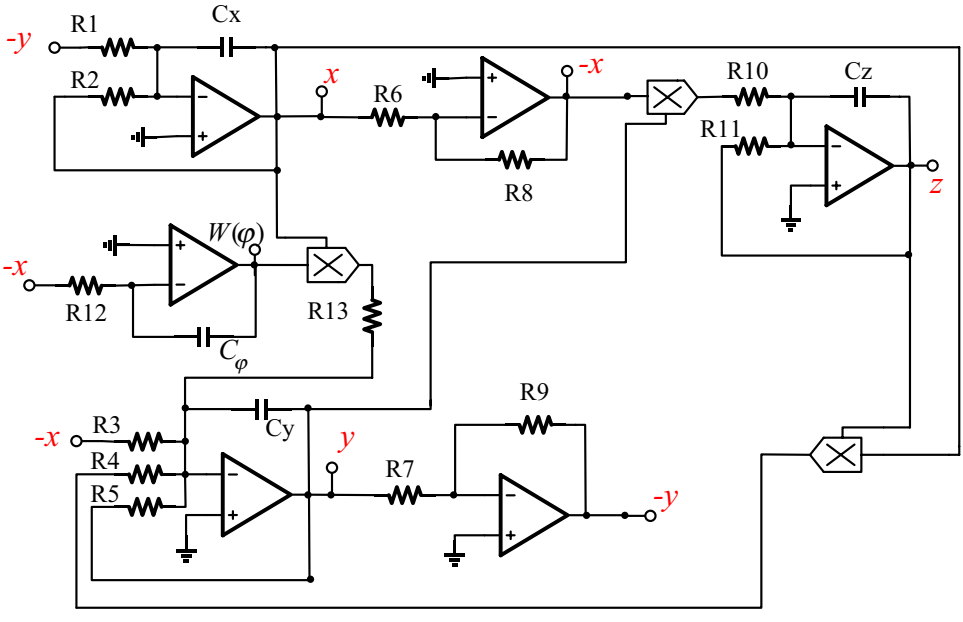

Fig. 13. Circuit diagram for system (14).

operations of addition, subtraction and integration. Multiplication operation is performed by the analog multiplier AD633. Since AD633 provides an overall scale factor of 1/10 V, a factor 0.1/V needs to be put on each multiplication. At the same time, AD633JN has laser-trimmed accuracy between −10 V and 10 V. However, the values of x, y and z, and φ in Fig. 6 may exceed this range. We must have a

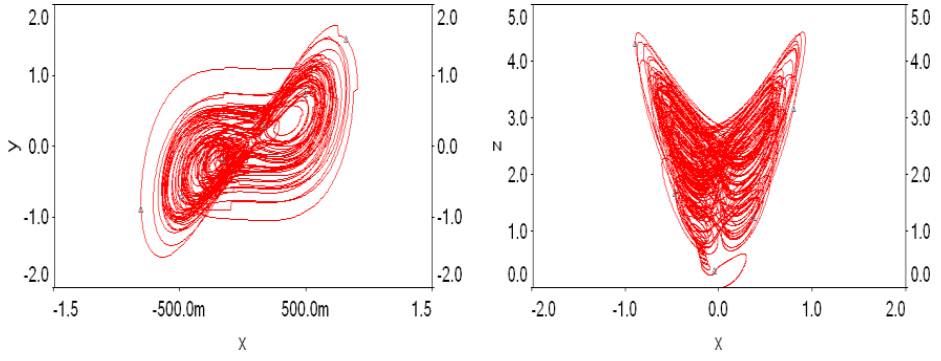

Fig. 14. Phase portraits of system (14) observed from Multisimsimulation. (a) Projection on x–y plane. (b) Projection on x–z plane. (c) Projection on y–z plane. (d) Projection on y–φ plane.

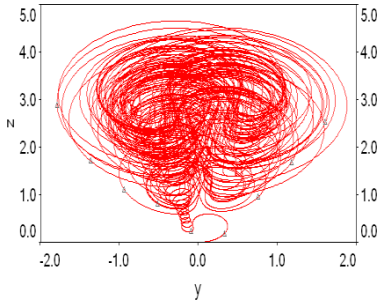

(c)

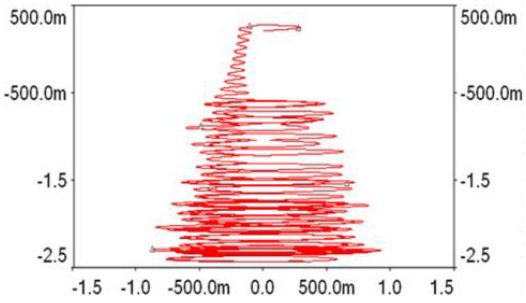

(d)

Fig. 14. (*Continued*)

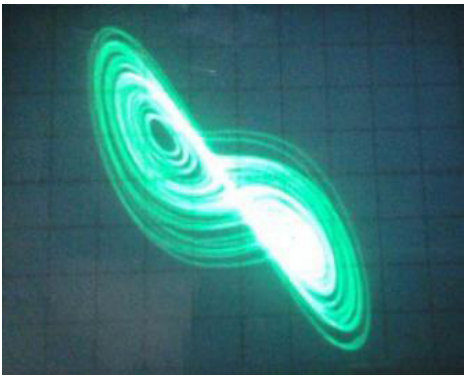

(a)

(b)

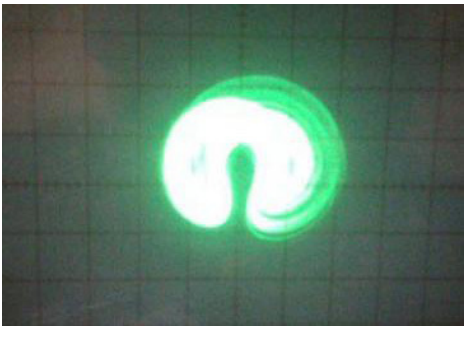

(c)

(d)

Fig. 15. Phase portraits of system (14) observed from oscilloscope. (a) Projection on x–y plane. (b) Projection on x–z plane. (c) Projection on y–z plane. (d) Projection on y–φ plane.

scale transform. The corresponding circuit equation can be described as

$$\begin{cases} \dot{v}_x = \dfrac{1}{C_x}\left(\dfrac{v_y}{R_1} - \dfrac{v_x}{R_2}\right), \\ \dot{v}_y = \dfrac{1}{C_y}\left(\dfrac{v_x}{R_3} - \dfrac{v_y}{R_5} - \dfrac{v_x v_z}{R_4} - \dfrac{v_x W(\varphi)}{R_{13}}\right), \\ \dot{v}_z = \dfrac{1}{C_z}\left(-\dfrac{v_z}{R_{11}} + \dfrac{v_x v_y}{R_{10}}\right), \\ \dot{v}_\varphi = \dfrac{1}{R_{12} C_\varphi} v_x \,. \end{cases} \tag{17}$$

When $C_x = C_y = C_z = C_\varphi = 10\,\text{nF}$, $R_1 = R_2 = 100\,\text{k}$, $R_6 = R_7 = R_8 = R_9 = 10\,\text{k}$, $R_{11} = R_{12} = 125\,\text{k}$, $R_3 = 33.333\,\text{k}$, $R_5 = 500\,\text{k}$, $R_4 = R_{10} = R_{13} = 20\,\text{k}$, the results of the circuit experiment are shown in Fig. 10, which are well consistent with the results of the numerical simulations shown in Fig. 6 and the Multisim simulations shown in Fig. 14. The experimental results in Fig. 15 have verified that the main idea about the memristive hyper-chaotic circuit of this paper is effective.

6. Conclusion

In this paper, a new simple memristor model was proposed. Then a hyper-chaotic system was proposed by adding a flux-controlled memristor with liner memductance. The 4D memristive system can generate a hyper-chaotic attractor, transient chaotic attractor, multiple attractors. Some basic properties of the new system have been investigated in terms of equilibria, hyper-chaotic attractors, Lyapunov exponent spectrum and bifurcation diagram. The results of experiment are well consistent with the numerical simulation results. The hyper-chaotic circuit based on memristor with linear memductance has simple circuit structure and easy implement, which can widely be used in chaotic secure communication, image encryption and other fields.

Acknowledgments

This work is supported by the National Natural Science Foundation of China (No. 61571185), The Natural Science Foundation of Hunan Province, China (No. 2016JJ2030) and the Open Fund Project of Key Laboratory in Hunan Universities (No. 15K027). The authors would like to thank the editors and anonymous reviewers for providing valuable comments which helped in improving the paper.

References

1. L. O. Chua, Memristor — The missing circuit element, *IEEE Trans. Circuit Theory* **18** (1971) 507–519.
2. D. B. Strukov *et al.*, The missing memristor found, *Nature* **453** (2008) 80–83.

3. J. M. Tour and T. He, Electronics: The fourth element, *Nature* **453** (2008) 42–43.
4. L. N. Jia, A. P. Huang and X. H. Zheng, Progress of memristor modulated by interfacial effect, *Acta Phys. Sin.* **61** (2012) 217306.
5. Y. V. Pershin and M. D. Ventra, Practical approach to programmable analog circuits with memristors, *IEEE Trans. Circuits and Systems I* **57** (2010) 1857–1864.
6. Q. F. Xia, W. Robinett and S. Williams, Memristor-CMOS hybrid integrated circuits for reconfigurable logic, *Nano Lett.* **9** (2009) 3640–3645.
7. M. Di Ventra, Y. V. Pershin and L. O. Chua, Circuit elements with memory: Memristors, memcapacitors, and meminductors, *Proc. IEEE* **97** (2009) 1717–1724.
8. J. Borghetti, Z. Y Li and R. S. Williams, A hybrid nanomemristor logic circuit capable of self-programming, *Proc. Natl. Acad. Sci. USA* **106** (2008) 1699–1703.
9. D. H. Song, X. Ren and Y. X. Zu, Basic properties and applications of the memristor circuit *Acta Phys. Sin.* **61** (2012) 118101.
10. S. Hasan and U. Cam, First-order memristor-capacitor filter circuits employing HP memristor, *J. Circuits Syst. Comput.* **28** (2014) 1450116.
11. M. Itoh and L. O. Chua, Memristor oscillators, *Int. J. Bifurcation Chaos* **18** (2008) 3182–3206.
12. B. Muthuswamy and P. P. Kokate, Memristor-based chaotic circuits, *IETE Tech. Rev.* **26** (2009) 417–429.
13. S. P. Wen, Z. G. Zeng and T. W. Huang, Adaptive synchronization of memristor-based chua's circuits, *Phys. Lett. A* **376** (2012) 2775–2780.
14. Z. H. Lin and H. X. Wang, Efficient image encryption using a chaos-based PWL memristor, *IETE Tech. Rev.* **27** (2010) 318–325.
15. Z. J. Li and Y. C. Zeng, A memristor oscillator based on a twin-T network, *Chin. Phys. B* **22** (2012) 040502.
16. A. M. A. EI-Sayed, A. EIsaid and H. M. Nour *et al.*, Dynamical behavior, chaos control and synchronization of a memristor-based ADVP circuit, *Commun. Nonlinear Sci. Numer. Simul.* **18** (2013) 148–170.
17. X. Y. Wang, G. Y. Wang and X. Y. Wang, Dynamic character analysis of a LDR, memristor-based chaotic system, *J. Circuits Syst. Comput.* **23** (2014) 1450085.
18. Q. H. Hong, J. F. Zeng and Y. C. Zeng, Design and simulation of a memristor chaotic circuit based on current feedback op amp, *Acta Phys. Sin.* **63** (2014) 185052.
19. B. C. Bao, Z. Liu and J. P. Xu, Dynamical analysis of memristor chaotic oscillator, *Acta Phys. Sin.* **59**(2010) 3785–3793.
20. Z. Liu, B. C. Bao and J. P. Xu, Transient chaos in smooth memristor oscillator, *Chin. Phys. B* **19** (2010) 030510.
21. B. C. Bao, Z. H. Ma and Q. Xu, A simple memristor chaotic circuit with complex dynamics, *Int. J. Bifurcation Chaos* **21** (2011) 2629–2645.
22. B. C. Bao, J. P. Xu and Z. Liu, Initial state dependent dynamical behaviors in a memristor based chaotic circuit, *Chin. Phys. Lett.* **27** (2010) 070504.
23. B. Muthuswamy and L. O. Chua, Simplest chaotic circuit, *Int. J. Bifurcation Chaos* **20** (2010) 1567–1580.
24. L. Zhou, C. H. Wang and L. L. Zhou, Generating hyperchaotic multi-wing attractor in a 4D memristive circuit, *Nonlinear Dyn.* **85** (2016) 2653–2663.
25. F. Y. Yang, J. L. Leng and Q. D. Li, The 4-dimensional hyperchaotic memristive circuit based on chua's circuit, *Acta Phys. Sin.* **63** (2014) 080502.
26. M. T. Abuelma'atti and Z. J. Khalifa, A new floating memristor emulator and its application in frequency-to-voltage conversion, *Analog Integr. Circuits Signal Process.* **86** (2016) 141–147.

27. Y. V. Persin and M. Di Ventra, Practical approach to programmable analog circuits with memristors, *IEEE Trans. Circuits Syst. I* **57** (2010) 1857–1864.
28. B. Muthuswamy, Implementing memristor based chaotic circuit, *Int. J. Bifurcation Chaos* **20** (2010) 1335–1350.
29. J. Kengne, Z. N. Tabekoueng, V. K. Tamba and A. N. Negou, Periodicity, chaos, and multiple attractors in a memristor-based Shinriki's circuit, *Chaos* **25** (2015) 103126
30. Q. Xu, Y. Lin, B. Bao and M. Chen, Multiple attractors in a non-ideal active voltage-controlled memristor based Chua's circuit, *Chaos Solitons Fractals* **83** (2016) 186–200.